行政院國家科學委員會專題研究計畫　成果報告

藉由結合檸檬酸鹽先驅物法與冷凍乾燥技術來製備鐵酸錳奈米粉體

計畫類別：個別型計畫
計畫編號：NSC92-2214-E-032-005-
執行期間：92 年 08 月 01 日至 93 年 07 月 31 日
執行單位：淡江大學化學工程與材料工程學系

計畫主持人：余宣賦

計畫參與人員：楊尚偉、張育綸、李柏澍

報告類型：精簡報告

處理方式：本計畫可公開查詢

中　華　民　國 93 年 10 月 11 日

藉由結合檸檬酸鹽先驅物法與冷凍乾燥技術來製備鐵酸錳奈米粉體

(Preparation of $MnFe_2O_4$ nanoparticles via a process combining the citrate precursor method and the frozen- drying technique)

計畫編號：NSC 92-2214-E-032-005-
執行期限：92 年 8 月 1 日至 93 年 7 月 31 日

主持人：余宣賦 (淡江大學 化材系)
計畫參與人員：楊尚偉、張育綸、李柏澍 (淡江大學 化材系)

摘要

次微米之 $MnFe_2O_4$ **結晶粉體可藉由火焰燃燒冷凍乾燥後之檸檬酸鹽先驅物來製得。檸檬酸加入水溶液中來螯合** Fe^{3+}**和** Mn^{2+}**，再經冷凍乾燥程序製得所需之固態先驅物。此固態先驅物經與火焰接觸來進行分解反應以生成所需之鐵酸錳細粉。製得之粉體以** XRD, TG, DSC, FT-IR, SEM, **和** SQUID **來進行特性分析。結果顯示在溶液酸鹼度等於或大於** 3 **時，所製得之** $MnFe_2O_4$ **粉體其晶粒尺寸為** 28.5 ± 1.2 nm**，且平均磁性為飽和磁場強度** 48.7 ± 1.5 emu/g**、殘留磁場強度** 13.4 ± 0.2 emu/g**、矯頑磁力** 55.7 ± 3.9 Oe**。**

關鍵詞：火焰燃燒、磁性粉體、鐵酸錳、檸檬酸鹽先驅物、冷凍乾燥

Abstract

Crystalline $MnFe_2O_4$ particles with sizes in submicrometers were produced by flame-combusting the freeze-dried citrate precursor. Aqueous solutions of nitrates, containing Fe^{3+} and Mn^{2+} chelated by citric acid, were freeze-dried. The freeze-dried citrate precursors were then thermally treated, using a butane-induced flame, to decompose organic constituents and to form ferrites. The resultant particles were characterized using XRD, TG, DSC, FT-IR, SEM, and SQUID. At pH ≥ 3, the fame-combusted specimens were composed of crystalline $MnFe_2O_4$ with average crystallite sizes of 28.5 ± 1.2 nm and exhibited magnetic characteristics of 48.7 ± 1.5 emu/g in magnetization measured at 1.5 kOe, 13.4 ± 0.2 emu/g in remanence magnetization, and 55.7 ± 3.9 Oe in coercive force.

Keywords: Flame Combustion, Magnetic Powder, Manganese Ferrite, Citrate Precursor, Freeze-drying

I. INTRODUCTION

To have high magnetic permeability, low magnetic losses, and proper mechanical properties, ferrites are interested in electronic industries. Ferrites with inverse spinel molecular structure are widely used for high-speed digital recording media or high-frequency transformers. The quality and performance of ferrite products are strongly influenced by their microstructures. To have better-controlled microstructure, the ferrite powder used in production should have the characteristics of high chemical homogeneity, ultrafine particle sizes with narrow size distribution, spherical-like shapes, and high sinterability. Several nonconventional techniques, such as coprecipitation [1-5], spray pyrolysis [6-9], sol-gel [10], hydrothermal [11-13], precursor [14-17], freeze-drying [18, 19], and combustion processes [20, 21], are used or under development to fulfill powder requirements.

Citrate precursor technique uses carboxylic groups of citric acid to chelate the required cations in a proper solution. Chelating metallic ions in the solution using trifunctional citric acid allows forming, after drying, a solid citrate precursor with uniformly distributed cations in the required ratio. Relative low pyrolyzing temperatures are required to form the corresponding oxides since all cations are mixed in molecular scale. Verma et al. [15] used a citrate precursor method to prepare nickel-zinic ferrites. They found that after sintering at 1373 K or above, the sintered nickel-zinic ferrites possessed higher electrical resistivities (≥ 10^8

Ωcm) than those prepared using traditional ceramic methods. Prasad and Gajbhiye [16] prepared ultrafine $NiFe_2O_4$ particles through pyrolyzing citrate precursors of Ni^{2+} and Fe^{3+} at different temperatures. Their experiments showed that $NiFe_2O_4$ completely crystallized at temperatures above 553 K and single domain particles with low saturation magnetization were found to form the linear chain like clusters because of strong magnetic dipolar interactions. The low saturation magnetization for these single domain particles was expected to be due to the spin noncollinearity predominantly at the surface. Gajbhiye and Balaji [17] studied thermal behavior of the citrate precursor to form $MnFe_2O_4$. They reported that three major steps involved in the decomposition of citrate precursor: the dehydration, the formation of intermediate acetonedicarboxylate complex, and the decomposition of acetonedicarboxylate to $MnFe_2O_4$ at 623 K.

By thermally decomposing freeze-dried (Li, Fe)-formates, Bonsdorf et al. [18] obtained $LiFe_5O_8$ powder at 973 K. At 523 K, (Li, Fe)-formates decomposed to form a reactive spinel phase similar to γ-Fe_2O_3 and at 573 - 973 K, Li^+ inserted into the γ-Fe_2O_3 lattices and reordered to form ferrite, without forming intermediate of α-Fe_2O_3. Bonsdorf et al. [19] also used the same technique to produce manganese ferrites and studied the effect of oxygen partial pressure at 673 - 1173 K on the phase stability and oxygen stoichiometry of manganese ferrite. At temperatures below 823 K and at high oxygen partial pressure, the formed ferrites were $MnFe_2O_{4+y}$ with y-value up to 0.5 corresponding to a γ-$(FeMn)_2O_3$ phase.

In recent years, combustion techniques are employed to produce ferrites. Fu and Lin [20] found that the saturation magnetization of Ni-Zn ferrite powder prepared by microwave-induced combustion can reach 59 emu/g after annealing at 1223 K for 4 h. Mangalaraja et al. [21] used a flash combustion technique to prepare Ni-Zn ferrite. After sintering, they found that the sintered ferrites possessed lower values for the dielectric constant and dielectric loss than those for the ferrites prepared by conventional ceramic method for the same composition.

In this study, citrate precursor method, freeze-drying, and flame-combustion technique were integrated to produce $MnFe_2O_4$. Effects of pH of the starting solution on the properties of combusted specimens were investigated. To reveal the vantage of flame-combustion technique, the freeze-dried specimens were also thermally treated in a muffle furnace with air atmosphere and the characteristics of resultant particles were compared with those of the combusted specimens.

II. EXPERIMENTAL

All chemicals used in this study were reagent purity and were used without further purification. $Mn(NO_3)_2 \cdot 6H_2O$ (99% purity, Showa, Japan), $Fe(NO_3)_3 \cdot 9H_2O$ (99% purity, Showa, Japan), and anhydrous citric acid (99.5% purity, Showa, Japan) in molar ratios of Mn^{2+} : Fe^{3+} : $C_3H_4(OH)(COOH)_3$ = 1 : 2 : 4.5 were dissolved in de-ionized water to form aqueous solutions of 0.12 M metallic ions concentration. Citric acid was to chelate metallic ions in the solution. After stirring for 30 min, the pH of solution was adjusted using $NH_4OH_{(aq)}$ (28 wt%, Echo, Taiwan). Four different pH conditions: ~1 (with no NH_4OH additions), 3, 7, and 9 were investigated in this study. To assure the complete chelation of metallic ions by citric acid, the solution was continuously stirred for 24 hr, followed by quickly freezing the solution. The frozen solution was then placed into a freeze-dryer (VD-500F, Taitec, Japan) to remove all volatile compounds. The freeze-dried solids so obtained were thermally treated, either by heating in a muffle furnace with air atmosphere and a heating rate of 5 K/min or by combustion using a butane-induced flame, to decompose organic constituents and to form ferrites.

The heated and combusted specimens were characterized using x-ray diffraction (XRD; D8A, Bruker, Germany), infrared spectroscopy (FT-IR; Magna-IR™ spectrometer 550, Nicolet, USA), scanning electron microscopy (SEM; S800, Hitachi, Japan), thermogravimetric analysis (TG; Ger-TGA 2950, Netzsch, Germany), and differential scanning calorimetric analysis (DSC; HT-DSC 404,

Netzsch, Germany). The crystallite sizes of $MnFe_2O_4$ in the obtained specimens were estimated by employing the Scherrer's formula in the profiles of (311) XRD peak of $MnFe_2O_4$. The measured IR absorption bands of the specimens were distinguished using the information published in Ref. 22. The magnetic characteristics of some selected specimens were measured at room temperature using a superconducting quantum interference device magnetometer (SQUID; MPMS 7, Quantum Design, USA). Effects of pH of the solution and heating conditions on the formation of manganese ferrite fine particles were investigated.

III. RESULTS AND DISCUSSION

A. Heating the freeze-dried specimens in a muffle furnace –

Figure 1 shows XRD patterns of the specimens obtained by heating the freeze-dried solids of different pH values to 473 K in a muffle furnace, using a heating rate of 5 K/min and a soaking time of 24 hr. While no crystalline phases were detected in the specimens of pH = ~1, 7, and 9, crystalline $MnFe_2O_4$ was appeared in the heated specimen of pH = 3. Figure 2 gives thermal curves of the freeze-dried specimen of pH = 3. Strong exothermic changes (DSC peak temperature at 478 K) accompanying with more than 43% weight loss occurred at temperatures between 458 and 503 K. At these temperature ranges, ammonium nitrate in the specimen was oxidized and heat was evolved, which accelerated the decomposition of organic constituents in the specimen and the formation of crystalline $MnFe_2O_4$. After 503 K, another exothermic reaction (DSC peak temperature at 576 K) took place and was ceased at about 646 K, which resulted in about 10.6% weight loss; hydrocarbon residuals were removed at this temperature range.

Although no other distinguishable peaks were detected in DSC curve after 646 K, slightly weight changes in TG curve were observed at temperature around 823 K (see magnified TG curve in Figure 2). At temperatures between 803 and 844 K, the specimen lost about 0.3% in weight and after

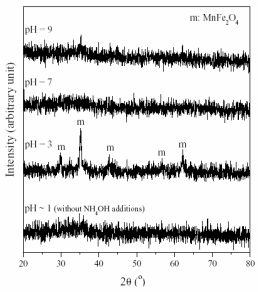

Figure 1. XRD patterns for the specimens obtained by heating the freeze-dried solids of different pH values in air at 473 K.

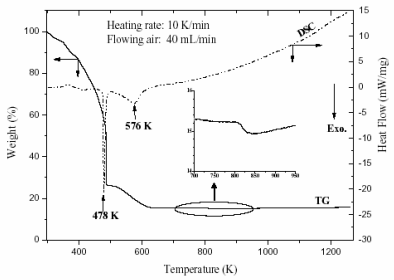

Figure 2. TG and DSC curves for the freeze-dried solids of pH = 3.

844 K the weight of specimen slowly increased with temperatures. 0.3% weight loss occurred at temperatures between 803 and 844 K should be mainly due to the oxidation of residual charcoals resulted from the incomplete oxidation of hydrocarbons in the specimen at lower temperatures. The increase of weight of the specimen after 844 K was ascribed to the oxidation of Mn^{2+} to form Mn^{3+}, which was evidenced from XRD analysis. Figure 3 shows XRD patterns and average crystallite sizes of $MnFe_2O_4$ for the specimens of pH = 3 at different heating temperatures. At 773 K and below, crystalline phase existed in the specimens was $MnFe_2O_4$ only. When the specimen was heated at 873 K, $MnFe_2O_4$ oxidized to form crystalline α-Fe_2O_3 and Mn_2O_3, which confirms the results observed from the TG curve in Figure 2 that after 844 K, the weight of specimen increases with temperatures. By comparing the corresponding crystallite sizes of $MnFe_2O_4$ at different temperatures, it shows that the average sizes of $MnFe_2O_4$ crystallites decreased with temperatures. This observation implied that at elevated temperatures $MnFe_2O_4$ are unstable in air and Mn^{2+} will first disintegrate from the surface of $MnFe_2O_4$ crystallites and tend to oxidize to form Mn^{3+}, resulting in size reduction of $MnFe_2O_4$

crystallites.

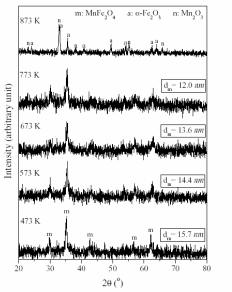

Figure 3. XRD patterns and $MnFe_2O_4$ crystallite size (d_m) for the specimens obtained by heating the freeze-dried solids of pH = 3 in air at five different temperatures, using a heating rate of 5 K/min.

B. Heating the freeze-dried specimens using a butane-induced flame -

The freeze-dried specimens of different pH were flame-combusted using a butane-induced flame and XRD patterns for these flame-combusted specimens are given in Figure 4. Crystalline $MnFe_2O_4$ was obtained regardless of pH used. Combustion by butane-induced flame caused the specimens to form crystalline manganese ferrite without oxidation of Mn^{2+} to Mn^{3+}. Through comparing average crystallite sizes of $MnFe_2O_4$ between those obtained at 473 K using a muffle furnace (e.g., d_m = 15.7 nm for the heated specimen of pH = 3) and those obtained by flame combustion (see d_m in Figure 4), it was found that combusting the specimens using butane-induced flame resulted in not only the formation of crystalline $MnFe_2O_4$ but also the growth of $MnFe_2O_4$ crystallites. It is suggested that butane-induced flame, in addition to provide high enough energy to decompose the organic constituents in specimens and to form crystalline manganese ferrite, created an oxygen-deficient environment to allow the formed $MnFe_2O_4$ crystallites to further grow bigger without the oxidation of Mn^{2+}.

While the average crystallite size of $MnFe_2O_4$ was about 17.4 nm for the combusted specimen without NH_4OH addition (i.e., pH = ~1), the combusted specimens with NH_4OH addition (i.e., pH = 3, 7, and 9) were composed of larger $MnFe_2O_4$ crystallites, having average crystallite sizes around 28.5 ± 1.2 nm. By adding NH_4OH into the aqueous solution of

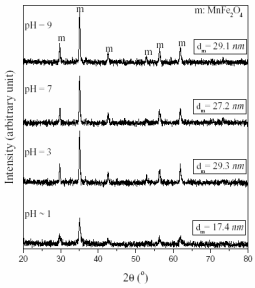

Figure 4. XRD patterns and $MnFe_2O_4$ crystallite size (d_m) for the specimens obtained by flame-combusting the freeze-dried solids of different pH values.

nitrates, ammonium ions reacted with nitrate ions to form NH_4NO_3, which remained in the specimen after freeze-drying. Upon contacting with butane-induced flame, ammonium nitrates uniformly distributed in specimens were instantaneously ignited and heat was evolved. The uniformly evolved heat caused the organic constituents in specimens to decompose more completely and enhanced the growth of $MnFe_2O_4$ crystallites. Figure 5 shows IR spectra of the freeze-dried specimens of pH = ~1 and 7 before and after flame combustion. Absorption bands for carboxylic groups (i.e., C=O stretching vibrations in 1740 - 1700 cm^{-1}, CO-O stretching in 1265 - 1205 cm^{-1}, and C-O stretching in 1190 - 1075 cm^{-1}) and for nitrate ions (asym. NO_3 stretching in 1410 - 1350 cm^{-1}) were detected for the freeze-dried solids of pH = ~1. For the freeze-dried solids of pH = 7, the absorption bands for NH_4^+ (absorbance at 3300 - 3030 cm^{-1} for N-H^+ stretching and at 1430 – 1390 cm^{-1} for N-H^+ deformation) were observed, in addition to the absorption bands for carboxylic groups and nitrate ions; it indicated the existence of ammonium nitrate in the freeze-dried specimen of pH = 7. After flame combustion, absorption bands for carboxylic groups, ammonium ions, and nitrate ions were no longer appeared in IR spectra of the combusted specimens but the absorption bands of C-H vibrations and C-C skeletal vibrations for alkane residues (i.e., asymmetric CH_3 stretching in 2985 - 2920 cm^{-1}, symmetric CH_3 stretching in 2880 - 2815 cm^{-1}, asymmetric CH_3 deformation in 1480 - 1430 cm^{-1}, symmetric CH_3 deformation in 1405 - 1355 cm^{-1}, and C-C rocking vibrations in 1130 - 1000 cm^{-1} and in 1060 - 900 cm^{-1}) were detected in the resultant particles of both pH = ~1 and pH = 7. It

indicated that some hydrocarbon residues still existed in the combusted specimens. By comparing the intensities of absorption bands of these alkane residues in the combusted specimens of pH = ~1 and 7, it was clear that the amounts of alkane residues existed in the combusted specimen of pH = 7 was much less than those existed in the combusted specimen of pH = ~1, indicating that ammonium nitrate formed by adding NH_4OH into the starting solution indeed enhanced the removal of organic constituents during flame combustion.

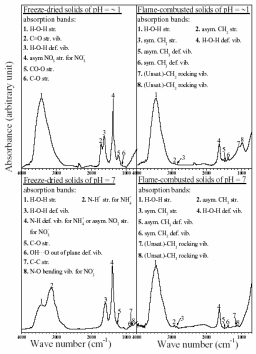

Figure 5. IR spectra for the freeze-dried solids and the flame-combusted solids of pH = ~1 and pH = 7.

Figure 6 gives SEM photomicrographs of the combusted specimens of pH = ~1, 3, 7, and 9, respectively. While larger agglomerated particles were obtained at pH = ~1, smaller particles with sizes in submicrometers were produced at pH = 3, 7, and 9. This indicated that the ignition of ammonium nitrates distributed in the specimen may also shatter the agglomerated particles and resulted in the formation of submicron $MnFe_2O_4$ particles. Table 1 summarizes magnetic characteristics of the combusted specimens of pH = ~1, 3, 7, and 9. The combusted specimen of pH = ~1 exhibited magnetization M(1.5 kOe) (magnetization measured at 1.5 kOe) of 29.9 emu/g, remanence magnetization M_r of 6.3 emu/g, and coercive force H_c of 47.6 Oe. With NH_4OH additions, the combusted specimens of pH = 3, 7, and 9 had average magnetic properties of 48.7 ± 1.5 emu/g in M(1.5 kOe), 13.4 ± 0.2 emu/g in M_r, and 55.7 ± 3.9 Oe in H_c. The magnetic characteristics were not well-developed for the combusted specimen of pH = ~1. At pH = 3 or above, the combusted specimens with larger $MnFe_2O_4$ crystallites exhibited much better magnetic characteristics than those obtained at pH = ~1. Crystallite sizes of $MnFe_2O_4$ affect the development of magnetic characteristics of $MnFe_2O_4$.

IV. CONCLUSIONS

Crystalline $MnFe_2O_4$ is unstable and tends to oxidize to form α-Fe_2O_3 and Mn_2O_3 in air at elevated temperatures. Although heating the citrate precursor of pH = 3 at 473 K in air could produce crystalline manganese ferrite, the crystallite sizes of $MnFe_2O_4$ were small, which will restrict the development of magnetic characteristics of manganese ferrite, and substantial amounts of the organic constituents still existed in the specimen. By flame-combusting the freeze-dried citrate precursors, crystalline $MnFe_2O_4$ particles can be produced regardless of the pH used. Adding NH_4OH into the starting solution and then flame-combusting the corresponding freeze-dried citrate precursors can produce larger $MnFe_2O_4$ crystallites with better-developed magnetic characteristics. At pH ≥ 3, the combusted specimens were composed of crystalline $MnFe_2O_4$ with average crystallite sizes of 28.5 ± 1.2 nm and exhibited magnetic characteristics of 48.7 ± 1.5 emu/g in M(1.5 kOe), 13.4 ± 0.2 emu/g in M_r, and 55.7 ± 3.9 Oe in H_c.

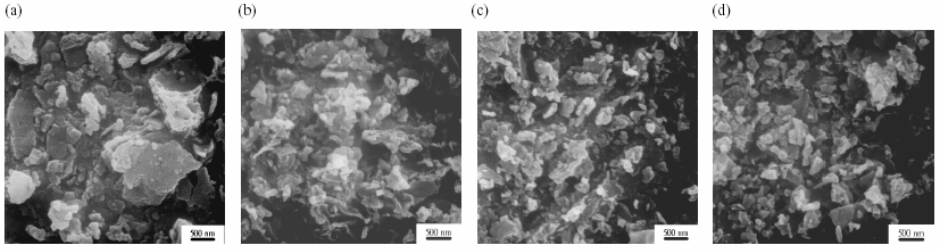

Figure 6. SEM photomicrographs for the specimens obtained by flame-combusting the freeze-dried solids of (a) pH = ~1, (b) pH = 3, (c) pH = 7, and (d) pH = 9.

Table 1. Magnetic characteristics of the flame-combusted specimens of different pH values

pH	Crystallite Sizes* d_m (nm)	Magnetization at 1.5 kOe M(1.5 kOe) (emu/g)	Remanence Magnetization M_r (emu/g)	Coercieve Force H_c (Oe)
~1	17.4	29.9	6.3	47.6
3	29.3	47.2	13.3	59.4
7	27.2	50.1	13.6	56.1
9	29.1	48.9	13.3	51.7

* average crystallite sizes of $MnFe_2O_4$ estimated from the XRD patterns using Scherrer's formula.

REFERENCES

1. Z.X. Tang and C.M. Sorensen, J. Colloid Interface Sci. **146** (1991) 38.
2. S. Rajendran and V.S. Rao, J. Mater. Sci. **29** (1994) 5673.
3. R.V. Upadhyay, K.J. Davies, S. Wells, and S.W. Charles, J. Magn. Magn. Mater. **139** (1994) 249.
4. S.P. Chaudhuri and I. Roy, Br. Ceram. Trans. **94** (1995) 250.
5. Q. Chen, A.J. Rondinone, B.C. Chakoumakos, and Z.J. Zhang, J. Magn. Magn. Mater. **194** (1999) 1.
6. D.W. Sproson, G.L. Messing, and T.J. Gardner, Ceeram. Int. **12** (1986) 3.
7. A.M. Gadalla and H. Yu, J. Mater. Res. **5** (1990) 2923.
8. C.H. Chao and P.D. Ownby, J. Mater. Sci. **30** (1995) 6136.
9. H. Yu and A.M. Gadalla, J. Mater. Res. **11** (1996) 663.
10. E. Mendelovici, R. Villalba, and A. Sagarzazu, J. Mater. Sci. **9** (1990) 28.
11. M.C. D'Arrigo, C. Leonelli, and G.C. Pellacani, J. Am. Ceram. Soc. **81** (1998) 3041.
12. W.H. Lin, S.K.J. Jean, and C.S. Hwang, J. Mater. Res. **14** (1999) 204.
13. C.W. Chang, Y.S. Hong, S.J. Wang, and I.N. Lin, Chin. J. Mater. Sci. **23** (1991) 62.
14. W. Zhong, W. Ding, Y. Jiang, N. Zhang, J. Zhang, Y. Du, and Q. Yan, J. Am. Ceram. Soc. **80** (1997) 3258.
15. A. Verma, T.C. Goel, R.G. Mendiratta, and R.G.. Gupta, J. Magn. Magn. Mater. **192** (1999) 271.
16. S. Prasad and N.S. Gajbhiye, J. Alloy Compou. **265** (1998) 87.
17. N.S. Gajbhiye and G. Balaji, Thermochimica Acta **385** (2002) 143.
18. G. Bonsdorf, H. Langbein, and K. Knese, Mater. Res. Bull. **30** (1995) 175.
19. G. Bonsdorf, K. Schäfer, K. Teske, H. Langbein, and H. Ullmann, Solid State Ionics **110** (1998) 73.
20. Y. Fu and C. Lin, J. Magn. Magn. Mater. **251** (2002) 74.
21. R.V. Mangalaraja, S. Ananthakumar, P. Manohar, and F.D. Gnanam, J. Magn. Magn. Mater. **253** (2002) 56.
22. G. Socrates, Infrared and Raman Characteristic Group Frequencies - Tables and Charts, 3rd ed. (John Wiley & Sons, New York, USA, 2001)